J Incl Phenom Macrocycl Chem (2009) 65:73–81
DOI 10.1007/s10847-009-9624-8

ORIGINAL ARTICLE

Fe-MCM-41 with highly ordered mesoporous structure and high Fe content: synthesis and application in heterogeneous catalytic wet oxidation of phenol

Dinh Quang Khieu · Duong Tuan Quang · Tran Dai Lam · Nguyen Huu Phu · Jae Hong Lee · Jong Seung Kim

Received: 16 June 2009 / Accepted: 22 June 2009 / Published online: 11 July 2009

Abstract Iron-substituted MCM-41 materials (Fe-MCM-41) have been synthesized via a hydrothermal method with in situ incorporation of Fe(III) oxalate complex under various basic conditions. The resulting Fe-MCM-41 samples were characterized by X-ray diffraction, N_2 adsorption measurement, and UV–Vis spectrometry. By controlling initial synthesized pH, the Fe-MCM-41 with highly ordered hexagonal mesoporous structures and high iron content (Si/Fe = 20) could be obtained. The iron species in Fe-MCM-41 samples mainly coexisted in isolated iron and highly dispersed iron oxide nanoclusters. Activity and stability of the obtained catalyst were evaluated on the wet peroxide oxidation of phenol under mild reaction conditions (<80 °C, ambient pressure). The Fe-MCM-41 with highly ordered mesoporous structure and high Fe content appeared to be the most interesting catalysts for phenol degradation owing to its high organic mineralization, low sensitivity to leaching Fe out and good oxidant efficiency.

Keywords Fe-MCM-41 · Catalytic wet peroxide oxidation · Heterogeneous Fenton-type catalyst

Authors dedicate this publication to Profs. Jack Harrowfield and Jacques Vicens in celebration of their 65th birthdays.

D. Q. Khieu · D. T. Quang
Hue University, Hue 84054, Vietnam

T. D. Lam · N. H. Phu
Vietnamese Academy of Science and Technology, Hanoi 8404, Vietnam

J. H. Lee · J. S. Kim (✉)
Department of Chemistry, Korea University, Seoul 136-701, Republic of Korea
e-mail: jongskim@korea.ac.kr

Introduction

Wet air oxidation (WAO) is a very attractive and useful technique for reducing the total organic carbon in industrial wastewater. WAO is usually practiced between 100–300 °C and at the pressures in the range of 1–10 MPa [1]. These severe reaction conditions can lead to high installation costs, and thus practical applications of this process are limited. The growing concern about the removal of pollutants from wastewater streams has stimulated the development of new treatment technologies to meet tightening regulations. In catalytic wet peroxide oxidation (CWPO) processes, the redox properties of dissolved transition metals are used to generate hydroxyl radicals under mild reaction conditions with the presence of hydrogen peroxide [2]. However, the limited range of the pH (3–5) at which the reaction proceeds more successfully and the need of recovery of the homogeneous catalyst are major drawbacks of this technology. These drawbacks can be overcome in principle by using a heterogeneous Fenton type catalyst such as iron-containing zeolites and clays [3, 4]. But zeolites also have resistance to the diffusion of organic contaminants into them if the molecular size of organic contaminants is greater than the pore size of zeolites.

In 1991, the synthesis of a new family of mesoporous molecular sieves designated as M41S attracted worldwide interest in many areas of physical, chemical and engineering sciences [5–7]. The mesoporous molecular sieve MCM-41 (a member of the M41S family) possesses a hexagonally arranged uniformed pore structure and large specific surface area, which makes it a very promising as a catalyst, catalyst support, or adsorbents [8, 9]. The incorporation of transition metal ions into the framework sites of molecular sieve MCM-41 has provided various catalytic

materials [10, 11]. Among them, iron containing mesoporous materials are of particular interest thanks to their unique catalytic properties in various reactions [12, 13]. Fe-MCM-41, which have redox properties, are expected to enhance intraparticle diffusion when compared to microporous zeolite materials with its special characteristics such as higher surface area together with large pore size. However, it is very difficult to introduce the iron ions into MCM-41 due to its rapid hydrolysis in alkaline medium forming large iron oxide particles. As a result, it might reduce the positive textural properties of catalysts. Hence, many attempts both to increase amount of iron ions into MCM-41 and to improve textural properties of the mesoporous structures have been made. Wingen et al. [14] showed that the incorporation of iron in the form of $K_4[Fe(CN)_6]$ into MCM-41 seems to enhance the textural properties of Fe-MCM-41, however, the incomplete introduction of iron into silica framework is inevitable because of the solubility of $[Fe(CN)_6]^{4-}$ complex in alkaline medium. Gokulakrishnan et al. [15] posited that the synthesis of Fe-MCM-41 with molar ratio of Si/Fe = 32 has high surface area and highly ordered mesoporous structures.

Wu et al. [16] reported a simple and effective method denoted "pH-adjusting" was used to graft a large amount of heteroatoms such as Al and Ti to mesoporous silica material SBA-15. From this point of view, the one-step incorporation of iron into MCM-41 or silicate may be controlled by the following two means: (a) covalent attachment where the complexes of iron were chemically bonded to the silica surface; (b) pH adjustment to certain values not so high to limit the precipitates of iron ions nor so low to reduce the likelihood of forming mesoporous structure of MCM-41.

Phenol is present in wastewater of various industries, such as pulp and paper industries and is classified as hazard chemicals [17]. Current methods for removing phenol from industrial waste waters include solvent extraction, microbial degradation, adsorption, CWPO [4, 17–19]. For the last case, catalytic metal containing materials such as Cu-SBA-15 [20], Ti-MCM-41 [21], Fe-MCM-41 [12], and diatomite minerals [22] only exhibit the limited oxidation of phenol to form catechol and hydroquinone (catechol/hydroquinone = 0.5–2). Few papers [23] have reported total oxidation of phenol to form inorganic acids using heterogeneous catalysts in CWPO processes.

In the present paper, one step-incorporation of iron to silica mesoporous MCM-41 by using Fe(III) oxalate as iron source and the pH adjustment of synthesized gel were presented. The catalytic oxidation of phenol in aqueous solution over obtained catalysts was also discussed.

Experimental procedure

Catalyst preparation

Fe-MCM-41 were synthesized using tetraethyl orthosilicate (TEOS, Merck) and ferric nitrate ($Fe(NO_3)_3{\cdot}9H_2O$, Merck) as silicon and iron precursors, respectively. Cethyltrimethyl ammonium bromide (CTAB, Aldrich) was used as the structured –directing agent. Five different catalysts with molar ratio of Si/Fe = 20 in synthesized gel were prepared in different pH media. In a typical synthesis: 1.78 g of CTAB was dispersed in m_w (g) of distilled water under stirring to obtain a homogeneous solution. On the other hand, another homogeneous solution was prepared by mixing 9.4 g of TEOS with the solution of 0.9129 g of $FeNO_3{\cdot}9H_2O$, 1.1388 g of $H_2C_2O_4{\cdot}2H_2O$ and 10 g of distilled water. Next, the solution of TEOS and iron salt were added to the solution of CTAB with stirring, just after, m_{alk} (mL) of solution of 1 M NaOH was added to form a gel for 4 h and the gel was kept under moderate stirring condition for additional 24 h. The amount of m_w and a_{alk} was presented in Table 1.

The gel was transferred into Teflon bottle and heated to the temperature of 100 °C for the aging time of 24 h. After cooling to ambient temperature, the solid was collected by filtering, washing and drying at 100 °C. Finally, solid was calcined at 550 °C for 10 h to remove organic surfactant. The calcined samples were designated as Fe-MCM-41(6.3), Fe-MCM-41(7.2), Fe-MCM-41(10.7), Fe-MCM-41(11.0), and Fe-MCM-41(11.2) where numbers in brackets were denoted as the value of pH in the filtrate. Since the filtrate is free of iron ions (indicated by KSCN) for all samples the molar ratio of Si/Fe = 20 in the synthesized gel is supposed to be equal to that of calcined sample. In addition, MCM-41 was synthesized by above mentioned procedure without iron oxalate complex added.

Table 1 The pH value of the filtrate and the amount of distilled water (m_w) and alkaline solution (m_{alk})

Sample	Molar ratio of Si/Fe synthesized gel	pH of filtrate	Distilled water, m_w (mL)	1 M NaOH, m_{alk} (mL)
Fe-MCM-41(6.3)	20	6.3	134.7	21.3
Fe-MCM-41(7.2)	20	7.2	129.7	26.3
Fe-MCM-41(10.7)	20	10.7	111.0	45.0
Fe-MCM-41(11.0)	20	11.0	109.0	47.0
Fe-MCM-41(11.2)	20	11.2	100.0	56.0

Characterization methods

Nitrogen adsorption/desorption isotherms of calcined samples were obtained using Micromeritics at 77 K. The pore-size distribution (PSD) was determined by the Barrett–Joyner–Halenda (BJH) method from desorption isotherm data. The mesopore volume, V_{mes}, was obtained by integrating the PSD curves from pore size of 20 to the 500 Å. Mesoporous diameter (main channel), d_p was determined from the maximum peak of PSD plot. The mesoporous phases of Fe-MCM-41 were monitored by powder low-angle X-ray diffraction (XRD), recorded on 8D Advance Bucker, Germany with CuK_α radiation in the range of 2θ from 0.5 to 10° with a scan step size of 0.01° and a scan step time of 0.04 s. The length of the hexagonal "unit cell" a_o was calculated using the formula $a_o = \frac{2d_{100}}{\sqrt{3}}$ [24]. Pore wall thickness, t_w, was assessed by subtracting d_p from a_o. The pH values of filtrates without dilution separated from precipitates after aging were measured by pH meter (Denver Instrument) at room temperature. The elemental analysis was conducted by Atomic Absorption Spectrometry (AAS-3300-Perkin Elmer). UV–Vis diffuse reflectance spectra were recorded on JASCO V-550 UV/Vis spectrophotometer using $BaSO_4$ as matrix.

Catalytic activity

In oxidation experiments [3], the runs were made in a two-neck, 250 mL pyrex round-bottom flask. The flask was heated with a thermalstat. For a typical run, 100 mL of a known concentration of phenol, catalyst in powder form, and H_2O_2 solution were loaded into the flask and heated to the desired temperature. The mixture was stirred with magnetic stirrer. The aliquots of suspension were withdrawn during reaction and filtered in order to remove the catalyst. The analysis of samples was performed by high performance liquid chromatography (HPLC) (Class VP Shimadzu). The HPLC was equipped with C-18 column using mobile phase (acetonitrile:methanol:water = 1:1:8) and a UV detector operating at 254 nm. The identification of the main products including catechol, hydroquinone, oxalic acid, formic acid, acetic acid was further confirmed by using corresponding standard chemicals.

Results and discussion

Catalyst characterization

Figure 1 shows low angle XRD patterns of Fe containing MCM-41 materials which were synthesized at different pH values. It is observed that the sample obtained from lowest pH value (6.3) treatment shows no reflections and the

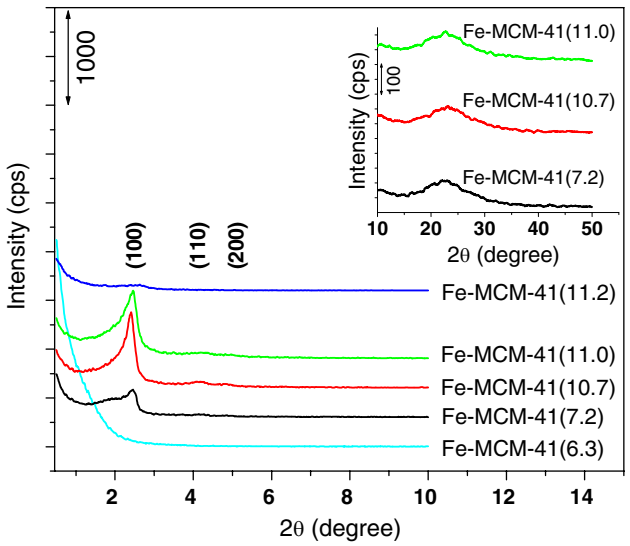

Fig. 1 XRD patterns of Fe-MCM-41 synthesized at different pH

intensities of reflections which are characteristic of mesoporous structure increase as synthesized pH increases. The sample (pH = 10.7) has well-resolved peaks of (100), (110), and (200) while the sample prepared at highest pH value (11.2) as well as lower pH value (pH <6.3) are unfavourable for maintaining the preformed mesostructure of MCM-41.

The introduction of iron ions into MCM-41 framework requires very strict conditions, indeed even small amounts of iron ions via ferric nitrate cause the collapse of preformed mesostructure MCM-41 due to the rapid hydrolysis of metal ions in basic media.

In the present work, the direct introduction of iron ions via iron oxalate complex $[Fe(C_2O_4)_3]^{3-}$ aims to retard the hydrolysis of iron ions. MCM-41 materials are synthesized under basic conditions via S^+I^- type [25], hence modified reaction pathway based on charge interactions may be conducted via $S^+(X^-M^{n+})I^-$ where M^{n+} is Fe^{3+}, S^+ cationic quaternary ammonium surfactant (CTA^+), I^- anionic silicate species, X^- oxalate. Due to the alkaline conditions during the synthesis of MCM-41 materials the iron(III) is precipitated as $Fe(OH)_3$ in the synthesis gel. These hydroxide precursors are in equilibrium with aqueous ferric ions, as expressed by this equation

$$Fe(C_2O_4)_3{}^{3-}(aq) + 3OH^- \rightleftharpoons Fe(OH)_3(solid) + 3C_2O_4{}^{2-}. \quad (1)$$

The iron hydroxide precursors are incorporated into silica framework, while the iron–oxalate complex remains dissolved. The obtained iron contents in the samples are therefore pH dependent. On the other hand, template CTAB exchanges ion with iron oxalate complex anion

$$Fe(C_2O_4)_3^{3-} + 3CTA^+Br^- \rightleftharpoons Fe(C_2O_4)_3(CTA)_3 + 3Br^-. \quad (2)$$

There is also another pH dependent equilibrium in synthesized gel [26]

$$SiO_2(OH)_2^{2-}(aq) + H^+ \rightleftharpoons SiO(OH)_3^-(solid). \quad (3)$$

The divalent silica species, which only exist in solution in significant amounts of about pH 12, are very soluble and do not polymerize and precipitate into the mesoporous framework. Only the monovalent silica species precipitate and form the mesoporous structure [26], the obtained amount of precipitated silica material is therefore pH dependent. Thus, the mesoporous structures of synthesized materials are dependent upon pH value of media as seen in Fig. 1. The OH^- concentration greatly affects the charge density on the silica surface, which influences the obtained structure of the synthesized materials as the surfactants self-assemble into the mesoporous structure that provides the best match to charge density on silica surface. All the equilibria in Eqs. 1–3 above affect the charge density matching process: through by the amount of aqueous iron ions in solution, and by the amount of the precipitated silica phase, respectively. Therefore, by controlling all these equilibria, the obtained structures and the iron content in the samples may be simultaneously controlled.

In the wide-angle region (the inset of Fig. 1) no reflection peak corresponding to crystalline iron oxides could be observed. Possibly, iron species were introduced into the framework of ordered mesoporous silica or particles of iron oxides in the sample were too small to be detected by X-ray diffraction.

To make the point clear, we analyzed the sample by using UV–Vis spectroscopy since it is an effective tool to determine the coordination environment of iron species in different materials.

Generally, the absorption band below 300 nm is attributed to isolated iron species and the absorption band between 300 and 600 nm is attributed to iron oxide nanoclusters, bulk iron oxide exhibits the absorption band between 400 and 600 nm [12, 13, 15].

Figure 2 shows UV–Vis spectroscopy of Fe-MCM-41(10.7), Fe-MCM-41(6.3) and Fe-MCM-41(11.2). All the samples exhibited a strong broad absorption between 200 and 600 nm, indicating that, for example, the iron species in Fe-MCM-41(10.7) mainly existed as isolated iron species and partly iron oxide nanoclusters. Also, the as-synthesized samples were white in color, suggesting that no bulk iron oxide was present and that all the iron cations were probably incorporated into the framework during synthesis. After calcination the Fe-MCM-41(10.7) became off-white in color suggesting the presence of extra framework iron.

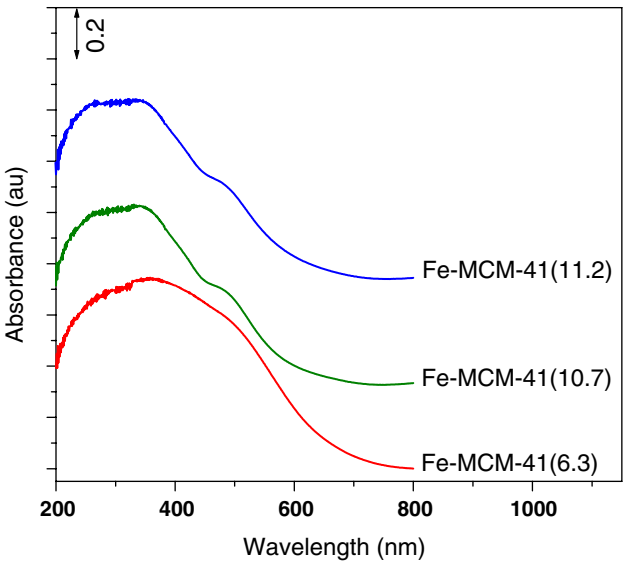

Fig. 2 UV–Vis spectra of synthesized Fe-MCM-41

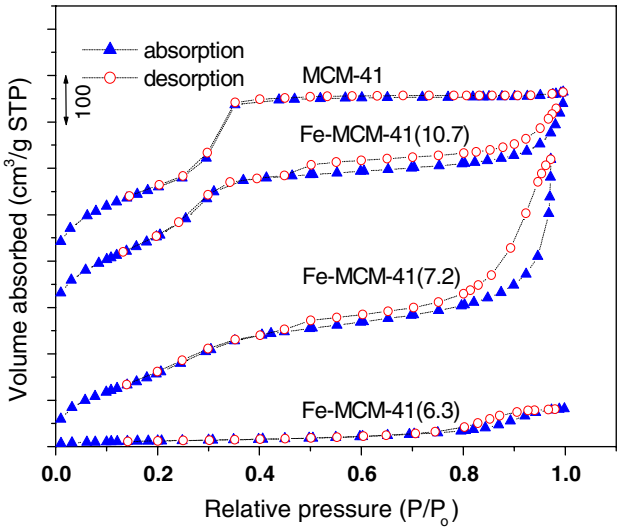

Fig. 3 Adsorption isotherms of Fe-MCM-41 synthesized with different concentrations of H^+ in gel

The pH effect on the textural properties of Fe-MCM-41 was evaluated by nitrogen physisorption as shown in Fig. 3. In Fig. 3, there are dramatic changes in the isotherms of the samples synthesized at different initial pH. For MCM-41 and Fe-MCM-41(10.7), the N_2 adsorption isotherms corresponded to typical type *IV* [27]. This means that they exhibit uniform hexagonal mesoporous structure. Their condensation steps are sharp at p/p_o of $\sim$0.3 while condensation step of Fe-MCM-41(7.2) becomes unclear and one of Fe-MCM-41(6.3) could not be observed. These results indicate that a mesoporous structure increases in the order of MCM-41 > Fe-MCM-41(10.7) > Fe-MCM-41(7.2) > Fe-MCM-41(6.3). The adsorption data also

showed that the S_{BET} value decreases with the same order of the degree of ordered mesoporous structure (Table 2). The sample Fe-MCM-41(10.7) with high surface area, uniform mesoporous structure, and high iron content may expect excellent catalytic activity.

Catalytic activity in phenol oxidation and formal kinetics

Figure 4 presents a comparison of the activities of the catalysts prepared. In the case without catalyst the phenol conversion is only around 5% after 120 min whereas it increases significantly as catalyst is used. The catalysts can be ranked as follows in terms of activity in phenol oxidation Fe-MCM(10.7) > Fe-MCM-41(11.0) > Fe-MCM-41(7.2) > Fe-MCM-41(6.3).

It can be seen that the catalyst of Fe-MCM-41(10.7) is the most active one. The lowest activity of the catalyst Fe-MCM-41(6.3) should be related to its very low surface area and amorphous silica structure. It seems that the catalytic activity depends remarkably on the ordered hexagonal mesoporous structure. The more ordered and uniform the mesoporous structure, the higher the catalytic activity is. The highest ordered mesoporous structure of Fe-MCM(10.7) provides excellent catalytic activity.

In the present kinetic investigation, the H_2O_2 content in the liquid phase was maintained at an excessive level for complete oxidation of phenol. Hence, the H_2O_2 dependence of the CWPO reaction kinetics was avoided. The oxidation reaction kinetics can be represented by

$$\frac{dC}{dt} = -kC^n \tag{4}$$

where C is phenol concentration, k the reaction rate constant, t the time and n the order of reaction. For a first-order reaction ($n = 1$). Equation 4 is integrated to yield

$$\ln\left(\frac{C_o}{C}\right) = kt \tag{5}$$

in which C_o is the initial phenol concentration. According the above equation, a plot of $\ln(C_o/C)$ versus t will yield the reaction rate constant. Figure 5 displays such plots for Fe-MCM-41(10.7) at different temperatures. Apparently, two-stage, first-ordered reaction kinetics describes reasonably well the present catalytic CWPO treatment of phenol solution.

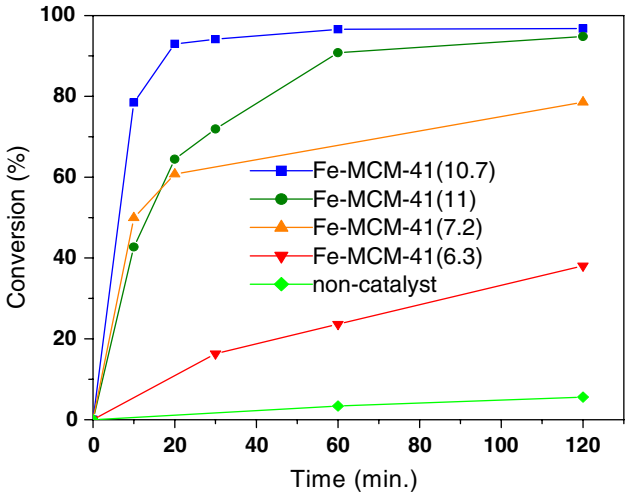

Fig. 4 Comparison between the catalytic activity over different Fe-MCM-41 catalysts reported as Fe-MCM-41(7.2), Fe-MCM-41(10.7), Fe-MCM-41(11.0), and Fe-MCM-41(11.2) (phenol: 2.5 g/L; catalyst: 0.01 g/L; H_2O_2: 0.588 mol/L; t°C = 70 °C)

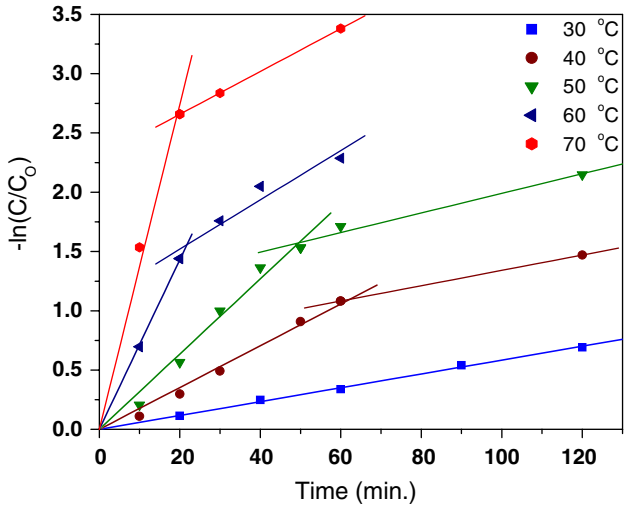

Fig. 5 Effect of reaction temperature on the conversion of phenol in catalytic wet peroxidation over Fe-MCM-41(10.7)

Table 2 Textural properties of MCM-41 and Fe-MCM-41 samples

Sample	D_{100} (Å)	a_o (Å)	d_{pore} (Å)	t_w (Å)	V_{mes} (cm^3 g^{-1})	S_{BET} (cm^3 g^{-1})
MCM-41	39.2	45.3	28.1	17.2	0.84	929.7
Fe-MCM-41(6.3)	–	–	–	–	–	44.4
Fe-MCM-41(7.2)	36.1	41.7	21.6	20.1	1.10	751.9
Fe-MCM-41(10.7)	36.8	43.5	25.4	18.1	0.90	886.6

Figure 5 shows that the transition time from the first-stage reaction to the second stage tends to decrease with an increase in the operating temperature. It is can be explained as follows: At a low temperature, the process occurs in the surface kinetic region

$$v = k_{\text{surface reaction}} C \tag{6}$$

where $k_{\text{surface reaction}}$ is rate constant of surface reaction.

When temperature increases, a breaking point appears in the plot of $\ln(C_o/C)$ versus t but it still observes linear plot with less sloop than that of the first stage indicating that the process would transfer from kinetically controlled region to diffusion-controlled one, then its rate constant must take account of both the diffusion ($k_{\text{diffusion}}$) and kinetic (k_{reaction}) steps [28, 29] so that

$$v = k_{\text{reaction}} C \tag{7}$$

where

$$k_{\text{reaction}} = \frac{k_{\text{diffusion}} k_{\text{surface reaction}}}{k_{\text{diffusion}} + k_{\text{surface reaction}}}.$$

Obviously,

$$k_{\text{reaction}} = \frac{k_{\text{surface reaction}}}{1 + \frac{k_{\text{surface reaction}}}{k_{\text{diffusion}}}} < k_{\text{surface reaction}}. \tag{8}$$

The reaction rate constants observed in Fig. 5 clearly reflect their dependence on the treatment temperature. Such dependence can be represented by the Arrhenius equation (9)

$$k = k_o \exp\left(-\frac{E}{RT}\right). \tag{9}$$

The reaction rates of the present catalyst CWPO process are strongly influenced by the catalyst dosage. Hence it would be of much interest to develop the correlations between the reaction rate constant and the catalyst dosage. Plots of $\ln(C_o/C)$ versus t for various Fe-MCM-41(10.7) dosages are shown in Fig. 6.

The catalyst dosage dependent rate constant of reaction kinetics is assumed to be described by the following mth order equation [29]

$$k = k_o W^m \tag{10}$$

where W is the catalyst dosage (mg/L) and m the order of catalyst dosage dependence. The logarithmic plot of k versus W is illustrated in Fig. 7. The slop of this plot provides the order of dependence (m). The value of m is equal to 0.9638 or approximately 1. The first order of the catalyst dosage dependence for the first-stage kinetics indicates that the Fe-MCM-41(10.7) possesses rather uniform surface properties.

In which E is the activation energy, k_o the frequency factor, R the gas constant and T the treatment temperature.

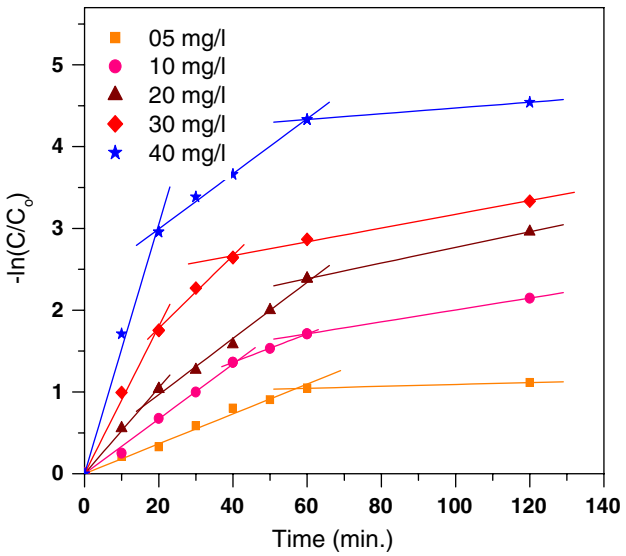

Fig. 6 Influence of catalyst dosage on the reaction kinetics of the catalytic CPWO process

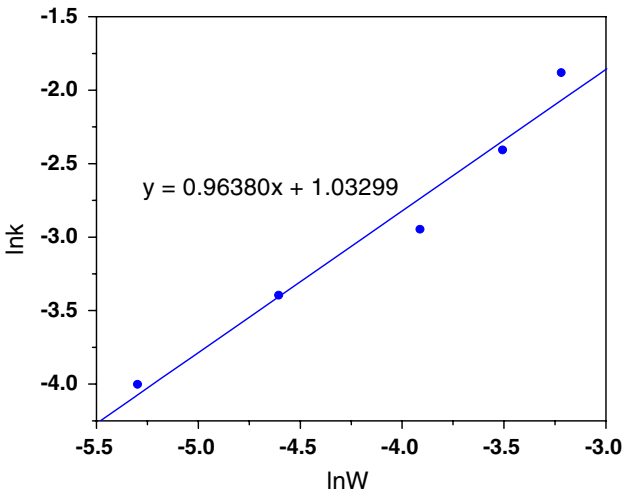

Fig. 7 Plot of lnk versus lnW at 70 °C

A plot of log k versus $1/T$ permits determinations of E. The activation energy obtained for the first stage is 15.9 kcal/mol. This value of E confirms that the CWPO reaction of phenol in the first stage occurs in the kinetic region (kinetic surface reaction).

Phenol oxidation reactions

It is well known that in the phenol oxidation process, in the first step, the phenol is oxidized to hydroquinone, catechol and small amount of benzoquinone and tar [4]. Subsequent oxidation of these products, after opening of the aromatic ring, leads to the formation of aliphatic carboxylic acids such as acetic acid, oxalic acid, and maleic acid.

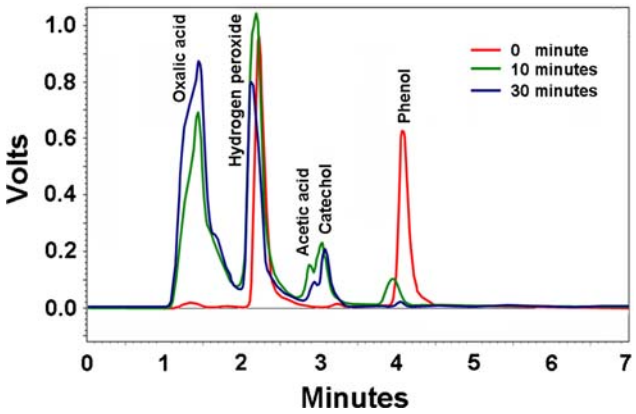

Fig. 8 Chromatography diagrams of phenol oxidized by H_2O_2 over Fe-MCM-41(10,7) catalyst (phenol: 2.5 g/L; catalyst: 0.01 g/L; H_2O_2: 0.588 mol/L; t°C = 70 °C)

Figure 8 shows chromatography diagrams of initial mixture of phenol and hydrogen peroxide and, the products of phenol oxidized at 10 and 30 min. The retention times of main components including oxalic acid, hydrogen peroxide, acetic acid, catechol, and phenol are around 1.4; 2.2; 2.8; 3.1; 4.0, respectively. The oxidation reaction occurs fast, converting phenol up to ca. 95% just after 30 min. It is noted that in the phenol oxidation using Fe-MCM-41(10.7) catalyst, firstly, catechol and back tarry materials are formed, and then further these products are converted to oxalic acid and small amount of acetic acid and formic acid. No benzoquinone and hydroquinone were detected as in [12, 30, 31]. We think that thermodynamically substitutions at both *ortho* and *para* position to form catechol and hydroquinone, respectively are possible. But, the main selectivity to catechol in this case shows that steric factors might play an important role. The steric constraints become more relevant when iron species are fitted within the MCM-41 channels and then, the reaction might go in a transition state, involving an iron complex with OH of phenol and OH radical of the peroxide. The reaction mechanism for the oxidation of phenol employing transition metals has been studied [3, 12, 30, 31].

To gain further insight the phenol oxidation of obtained Fe-MCM-41 catalyst the CWPO of hydroquinone and catechol was investigated separately. HPLC analyses show that main product of the CWPO of hydroquinone over Fe-MCM-41(10.7) catalyst is formic acid while that of catechol is oxalic acid. The reaction pathway proposed for the present study involves a first stage called "heterogeneous Fenton" where the interactions of Fe-MCM-41 catalyst with hydroperoxide yields HO* and HO_2* species via redox mechanism. Hydroquinone and catechol are subsequently obtained in parallel processes involving the attack of HO* radicals to aromatic ring as proposed by Franco et al. [30]. Benzoquinone can be obtained by the consecutive oxidation of hydroquinone. Subsequent oxidation of catechol and hydroquinone by HO* radicals produces oxalic acid and formic acid, respectively. Reaction pathway of phenol oxidation by hydrogen peroxide over Fe-MCM-41 is shown in Scheme 1. In the present work, the main dihydroxylphenol is catechol. It means that the reactions of (13) are prominent while those of (14) and (15) occur negligibly.

$$\mathrm{Fe^{3+}/MCM\text{-}41} + \mathrm{H_2O_2} \rightleftharpoons \mathrm{Fe^{2+}/MCM\text{-}41} + {}^{*}\mathrm{OOH} + \mathrm{H^{+}} \quad (11)$$

$$\mathrm{Fe^{2+}/MCM\text{-}41} + \mathrm{H_2O_2} \rightleftharpoons \mathrm{Fe^{3+}/MCM\text{-}41} + {}^{*}\mathrm{OH} + \mathrm{H^{+}} \quad (12)$$

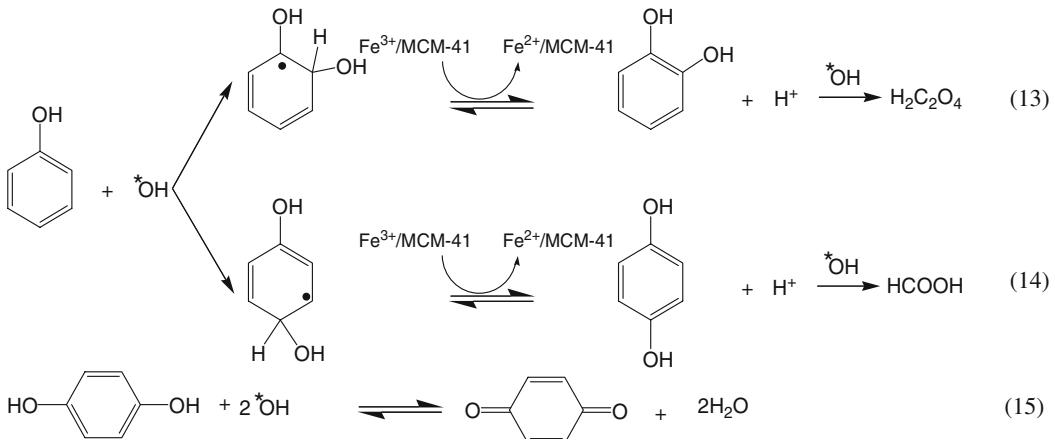

$$\mathrm{Fe^{3+}/MCM\text{-}41} + {}^{*}\mathrm{OH} + 2\mathrm{H_2O_2} \rightleftharpoons \mathrm{Fe^{2+}/MCM\text{-}41} + \mathrm{O_2} + \mathrm{H_2O} + \mathrm{H^{+}}. \quad (16)$$

Effect of solvents on phenol conversions was also investigated. As shown in Fig. 9, phenol conversion was ca. 100%

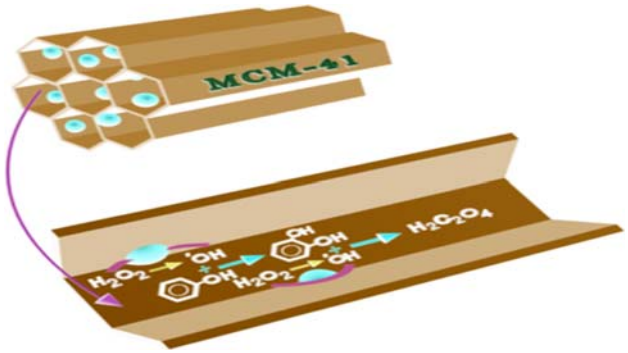

Scheme 1 Illustration of reaction pathway of phenol oxidation by hydrogen peroxide over Fe-MCM-41 catalyst

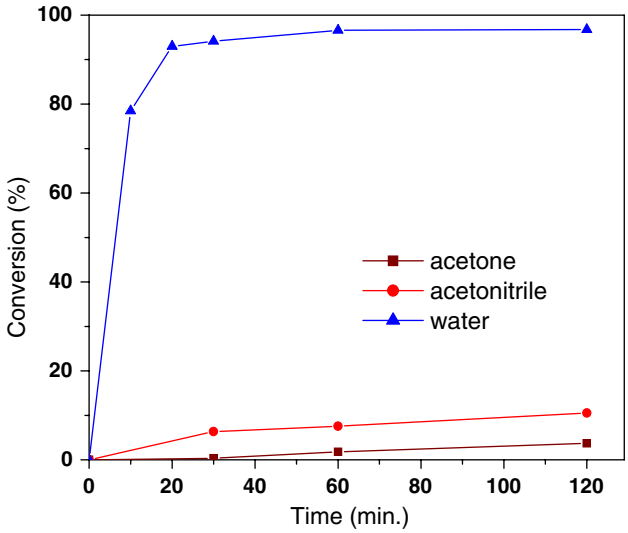

Fig. 9 Effect of solvents on phenol conversions at 70 °C over Fe-MCM-41(10.7)

in water and ca. 11% in acetonitrile. Phenol oxidation virtually did not proceed in acetone (less than 5%). In water, both phenol and H_2O_2, dissolved easily and active hydroxyl radicals can be formed effectively upon contact with Fe sites. This effect of solvents strongly supports that radical reaction mechanism is in operation in catalytic phenol oxidation over Fe-MCM-41. Radicals generated are more stable in polar solvents, and the polarity order of the solvents is water (1) > acetonitrile (0.65) > acetone (0.56), which is the same order as in phenol conversion obtained in this study.

Leaching experiment

During phenol oxidation process, the concentration of H^+ increases because of the formation of organic acids and in fact, pH of the reaction medium showed significant drop in pH from 6 to around 2.8 at the end of reaction. It can be conjectured that under this acidic condition iron species is partly removed from solids.

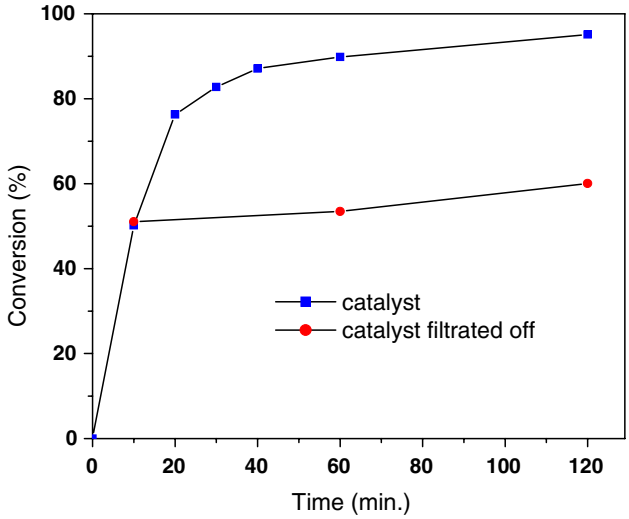

Fig. 10 Leaching experiment for phenol over Fe-MCM-41, the catalyst has been hot-filtrated off after 15 min

As the leaching of iron species could play an important role on the CWPO of phenol further catalytic studies were carried out as follows. The resultant solution after 15 min of reaction using Fe-MCM-41(10.7) as a catalyst was filtered in hot conditions to remove the catalyst. Figure 10 shows phenol conversion in the filtered solution compared with that carried out in presence of Fe-MCM-41(10.7).

The evolution of phenol conversion for filtered solution evidenced a very low activity in comparison with that shown by the heterogeneous catalytic system. After 120 min of reaction, phenol conversion increases from ~50 to 60% whereas that increased up to 90% for heterogeneous system with catalyst. Elemental analysis showed that almost 16% of Fe atoms have been removed from the framework (before Si/Fe ratio = 20, and after = 35). This data demonstrates beyond doubt that the activity of the solid catalysts is not due to only a homogeneous contribution of iron leached, but rather from the activity of heterogeneous catalyst.

Conclusions

Highly ordered mesoporous Fe-MCM-41 catalysts with up to 5 mol% Fe content were successfully synthesized by in situ incorporation of Fe(III) oxalate complex in terms of pH adjusting process. The obtained Fe-MCM-41 was found effective as catalyst in phenol oxidation. The final degradation product was mainly oxalic acid. It has been observed that during the reaction only a small amount of iron is leached from Fe-MCM-41. Hence, it can be concluded that wet hydrogen peroxide oxidation using a solid Fenton-type catalyst like Fe-MCM-41 may be a promising technology for treating aqueous solutions containing

organic contaminants. The proposed process of synthesized Fe-MCM-41 materials can be extended to apply to synthesize other Me-MCM-41 (Me: transition metal).

Acknowledgments This work was supported by the SRC (KOSEF) grant (No. R11-2005-008-00000-0) and the CRI Project of the MEST.

References

1. Sadana, A., Katzer, J.R.: Involvement of free radicals in the aqueous-phase catalytic oxidation of phenol over copper oxide. J. Catal. **35**, 140–152 (1974). doi:10.1016/0021-9517(74)90190-0
2. Chedeville, O., Bayraktar, A.T., Porte, C.: Modeling of Fenton reaction for the oxidation of phenol in water. J. Autom. Methods Manag. Chem. **2**, 31–36 (2005). doi:10.1155/JAMMC.2005.31
3. Calleja, G., Melero, J.A., Martinez, F., Molina, R.: Activity and resistance of iron-containing amorphous, zeolitic and mesostructured materials for wet peroxide oxidation of phenol. Water Res. **39**, 1741–1750 (2005). doi:10.1016/j.watres.2005.02.013
4. Ukrainczyk, L., McBride, M.B.: Oxidation of phenol in acidic aqueous suspensions of manganese oxides. Clays Clay Miner. **40**, 157–166 (1992). doi:10.1346/CCMN.1992.0400204
5. Vallet-Regí, M., Ruiz-González, L., Izquierdo-Barba, I., González-Calbet, J.M.: Revisiting silica based ordered mesoporous materials: medical applications. J. Mater. Chem. **16**, 26–31 (2006). doi:10.1039/b509744d
6. Witula, T., Holmberg, K.: Use of different types of mesoporous materials as tools for organic synthesis. J. Colloid Interf. Sci. **310**, 536–545 (2007). doi:10.1016/j.jcis.2007.01.060
7. Da Silva, J.P., Ferreira Machado, I., Lourenc, J.P., Vieira Ferreira, L.P.: Photochemistry of benzophenone adsorbed on MCM-41 surface. Microporous Mesoporous Mater. **84**, 1–10 (2005). doi:10.1016/j.micromeso.2005.05.012
8. Zhou, L., Liu, X., Sun, Y., Li, J., Zhou, Y.: Methane sorption in ordered mesoporous silica SBA-15 in the presence of water. J. Phys. Chem. B **109**, 22710–22714 (2005). doi:10.1021/jp056002
9. Kumar, D., Schumacher, K., du Fresne von Hohenesche, C., Grün, M., Unger, K.K.: MCM-41, MCM-48 and related mesoporous adsorbents: their synthesis and characterisation. Colloids Surf. A **187–188**, 109–116 (2001). doi:10.1016/S0927-7757(01)00638-0
10. Poh, N.E., Nur, H., Nazlan, M., Muhid, M., Hamdan, H.: Sulphated AlMCM-41: Mesoporous solid Brønsted acid catalyst for dibenzoylation of biphenyl. Catal. Today **114**, 257–262 (2006). doi:10.1016/j.cattod.2006.01.010
11. Selvaraj, M., Seshadri, K.S., Pandurangan, A., Lee, T.G.: Highly selective synthesis of trans-stilbene oxide over mesoporous Mn-MCM-41 and Zr–Mn-MCM-41 molecular sieves. Microporous Mesoporous Mater. **79**, 261–268 (2005). doi:10.1016/j.micromeso.2004.11.009
12. Choi, J.S., Yoon, S.S., Jang, S.H., Ahn, W.S.: Phenol hydroxylation using Fe-MCM-41 catalysts. Catal. Today **111**, 280–287 (2006). doi:10.1016/j.cattod.2005.10.037
13. He, N., Bao, S., Xu, Q.: Fe-containing mesoporous molecular sieves materials: very active Friedel-Crafts alkylation catalysts. Appl. Catal. A **169**, 29–36 (1998). doi:10.1016/S0926-860X(97)00347-5
14. Wingen, A., Anastasievic, N., Hollnagel, A., Werner, D., Schuth, F.: Fe–MCM-41 as a catalyst for sulfur dioxide oxidation in highly concentrated gases. J. Catal. **193**, 248–254 (2000). doi:10.1006/jcat.2000.2896
15. Gokulakrishnan, N., Pandurangan, A., Shinha, P.K.: Removal of citric acid from aqueous solution by catalytic wet peroxidation using effective mesoporous Fe-MCM-41 molecular sieves. J. Chem. Technol. Biotechnol. **82**, 25–32 (2007). doi:10.1002/jctb.1630
16. Wu, S., Han, Y., Zou, Y.C., Song, J.W., Zhao, L., Di, Y., Liu, S.Z., Xiao, F.S.: Synthesis of heteroatom substituted SBA-15 by the "pH-adjusting" method. Chem. Mater. **16**, 486–492 (2004). doi:10.1021/cm0343857
17. Tong, Z., Qingxiang, Z., Hui, H., Qin, L., Yi, Z.: Kinetic study on the removal of toxic phenol and chlorophenol from waste water by horseradish peroxidase. Chemosphere **37**, 1571–1577 (1998). doi:10.1016/S0045-6535(98)00140-4
18. Ming, Z.W., Long, C.J., Cai, P.B., Xing, Z.Q., Zhang, B.: Synergistic adsorption of phenol from aqueous solution onto polymeric adsorbents. J. Hazard. Mater. **128**, 123–129 (2006). doi:10.1016/j.jhazmat.2005.03.036
19. Santos, A., Yustos, P., Gomis, S., Ruiz, G., Ochoa, F.G.: Generalized kinetic model for the catalytic wet oxidation of phenol using activated carbon as the catalyst. Ind. Eng. Chem. Res. **44**, 3869–3878 (2005). doi:10.1021/ie050030g
20. Wang, L., Kong, A., Chen, B., Ding, H., Shan, Y., He, M.: Direct synthesis, characterization of Cu-SBA-15 and its high catalytic activity in hydroxylation of phenol by H_2O_2. J. Mol. Catal. A **230**, 143–150 (2005). doi:10.1016/j.molcata.2004.12.027
21. Kulawik, K., Schulz-Ekloff, G., Rathousky, J., Zukal, A., Had, J.: Hydroxylation of phenol over Ti-MCM-41 and TS-1. Collect. Czech. Chem. Commun. **60**, 451–456 (1995). doi:10.1135/cccc19950451
22. Han, W., Jia, Y., Xiong, G., Yang, W.: Diatomite as high performance and environmental friendly catalysts for phenol hydroxylation with H_2O_2. Sci. Technol. Adv. Mater. **8**, 106–109 (2007). doi:10.1016/j.stam.2006.11.015
23. Phu, N.H., Hoa, T.T.K., Tan, N.V., Thang, H.V., Ha, P.L.: Characterization and activity of Fe-ZSM-5 catalysts for total oxidation of phenol in aqueous solution. Appl. Catal. B **34**, 267–275 (2001). doi:10.1016/S0926-3373(01)00220-X
24. Vinu, A., Dhanashri, K.S., Hossain, K.Z., Ariga, K., Halligudi, S.B., Hartmann, M.: Direct synthesis of well-ordered and unusually Fe-SBA-15 mesoporous molecular sieves. Chem. Mater. **17**, 5339–5345 (2005). doi:10.1021/cm050883z
25. Soler-Illia, G.J., Sanchez, C., Lebeau, B., Patarin, J.: Chemical strategies to design textured materials: from microporous and mesoporous oxides to nanonetworks and hierarchical structures. Chem. Rev. **102**, 4093–4138 (2002). doi:10.1021/cr0200062
26. Brinker, C.J., Scherer, G.W.: Sol-Gel Science. Academic press, San Diego (1990)
27. Thang, H.V.: Synthesis, characterization, adsorption and diffusion properties of bi-porous SBA-15 and semi-crystalline UL-MFI mesostructured materials. Ph.D. thesis, University of Laval, Canada (2005)
28. Mukhlyonov, I.P., Gorshtein, A.E., Tumarkina, E.S., Tambovtseva, V.D.: Fundamentals of chemical technology. Mir Publishers, Moscow (1986)
29. Lin, S.H., Ho, S.J.: Catalytic wet-air oxidation of high strength industrial wastewater. Appl. Catal. B **9**, 133–147 (1996). doi:10.1016/0926-3373(96)90077-6
30. Franco, L.N., Perez, I.H., Pliego, J.A., Franco, A.M.: Selective hydroxylation of phenol employing Cu–MCM-41 catalysts. Catal. Today **75**, 189–195 (2002). doi:10.1016/S0920-5861(02)00067-6
31. Hu, X., Lam, F.L.Y., Cheung, L.M., Chan, K.F., Zhao, X.S., Lu, G.Q.: Copper/MCM-41 as catalyst for photochemically enhanced oxidation of phenol by hydrogen peroxide. Catal. Today **68**, 129–133 (2001). doi:10.1016/S0920-5861(01)00273-5